

1 **eTable 1 Characteristics of patients enrolled (Figure 6, A and B)**

Patient	Sex	Year sample collection	Diagnose at sample collection	anti-MOG antibody titer
1	n.a.	2018	TM	1:1000
2	F	2016	NMOSD	1:320
3	M	2016	NMOSD	1:1280
4	M	2016	Recurrent myelitis	1:320
5	n.a.	2017	TM	1:320
6	n.a.	2021	TM	1:100

2 TM =transverse myelitis; NMOSD = neuromyelitis optica spectrum disorder

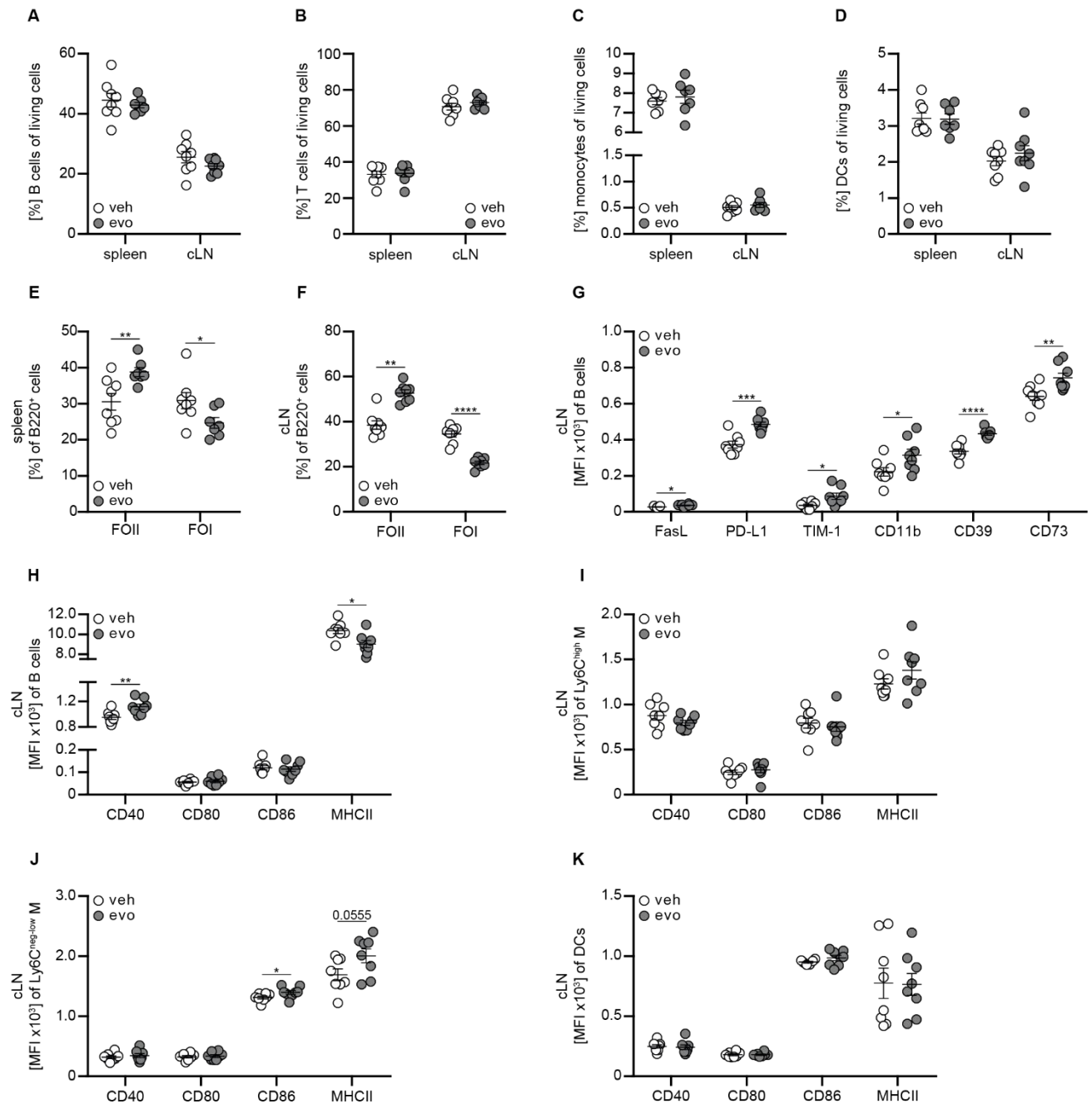
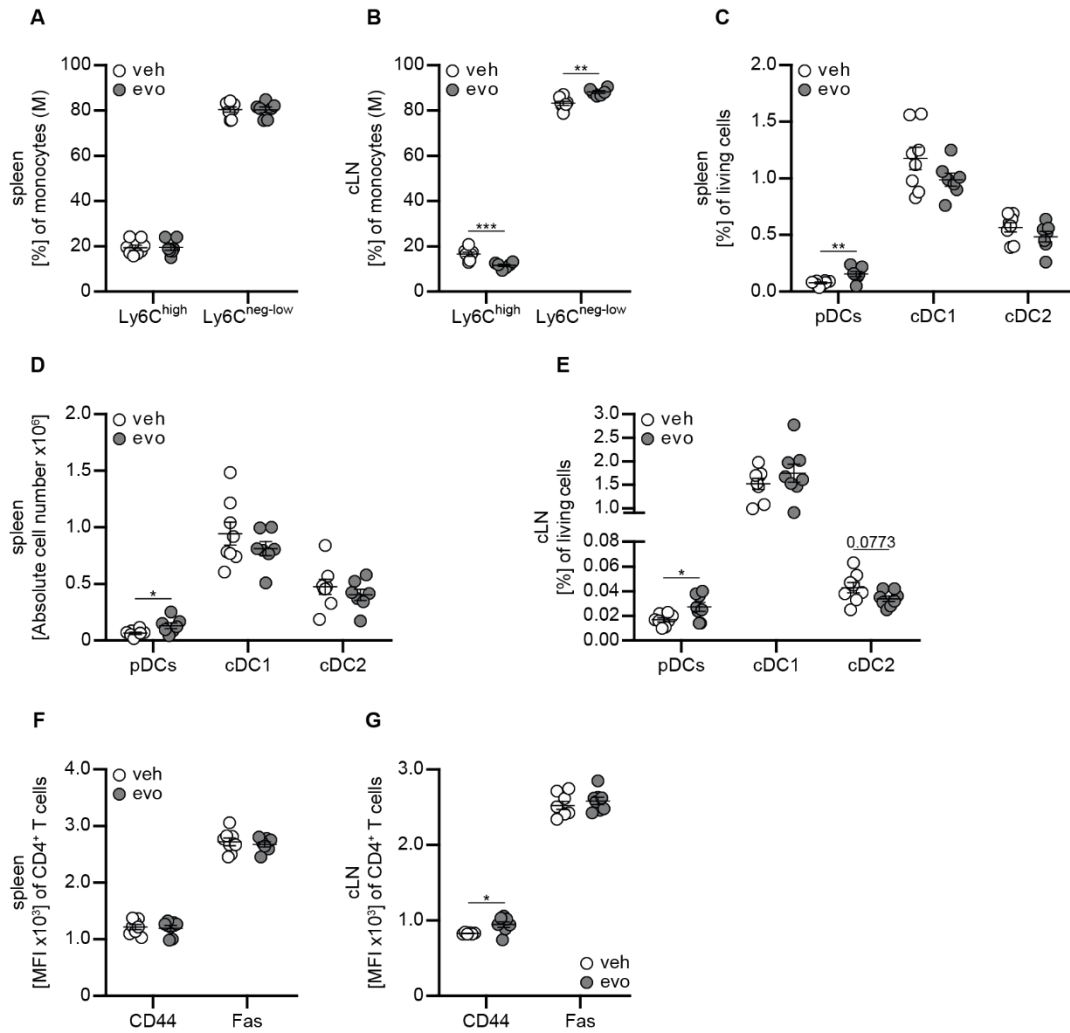


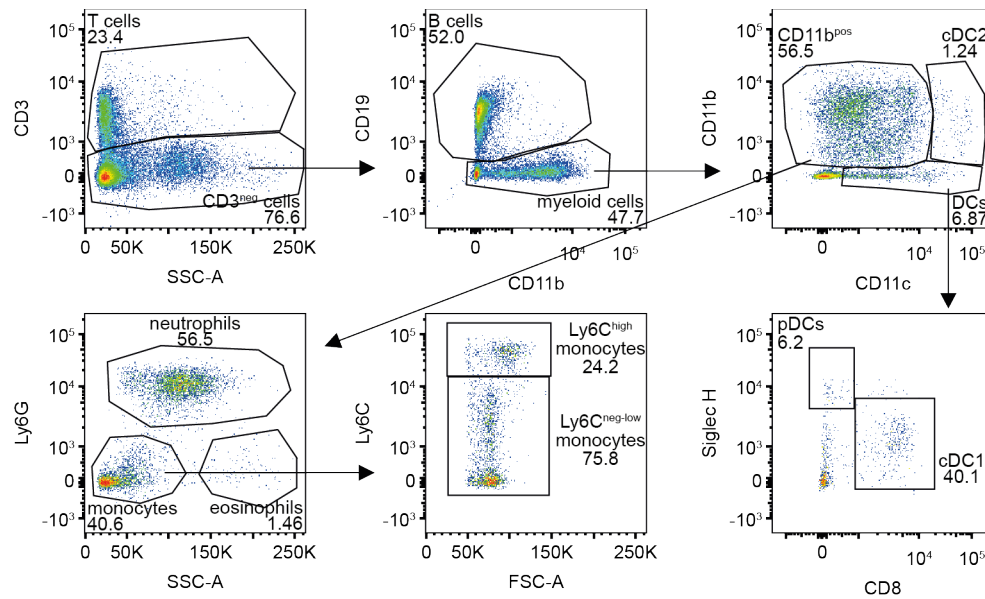
Figure 1 BTKi does not affect the frequencies of cell populations in the spleen nor the cervical lymph nodes. Naïve wildtype mice were treated daily with 3 mg/kg evobrutinib (evo) or vehicle control (veh) over a period of 21 days. Spleens and cervical lymph nodes (cLN) were analyzed via flow. Frequency of living cells in the spleen and cLN of **A** B cells (CD19⁺), **B** T cells (CD3⁺), **C** monocytes (CD11b⁺Ly6G⁻), and **D** dendritic cells (CD11b^{var}CD11c⁺). **E,F** Frequency of follicular (FO) B cells of B220⁺ cells in the spleen and cLN. **G** Mean fluorescence intensity (MFI) of molecules associated with regulatory properties analyzed on B220⁺ B cells. MFI of molecules associated with antigen presentation on **I** Ly6C^{high}, and **J** Ly6C^{neg-low} monocytes (M) and **K** dendritic cells (DCs) in the cLNs.

12 Data is shown as mean \pm SEM; n=7-8 and representative data of two independent experiments. Asterisks indicate significant difference
13 calculated using unpaired t test with Welch's correction or Mann-Whitney U test (*p<0.05, **p<0.01, ***p<0.001, ****p<0.0001).

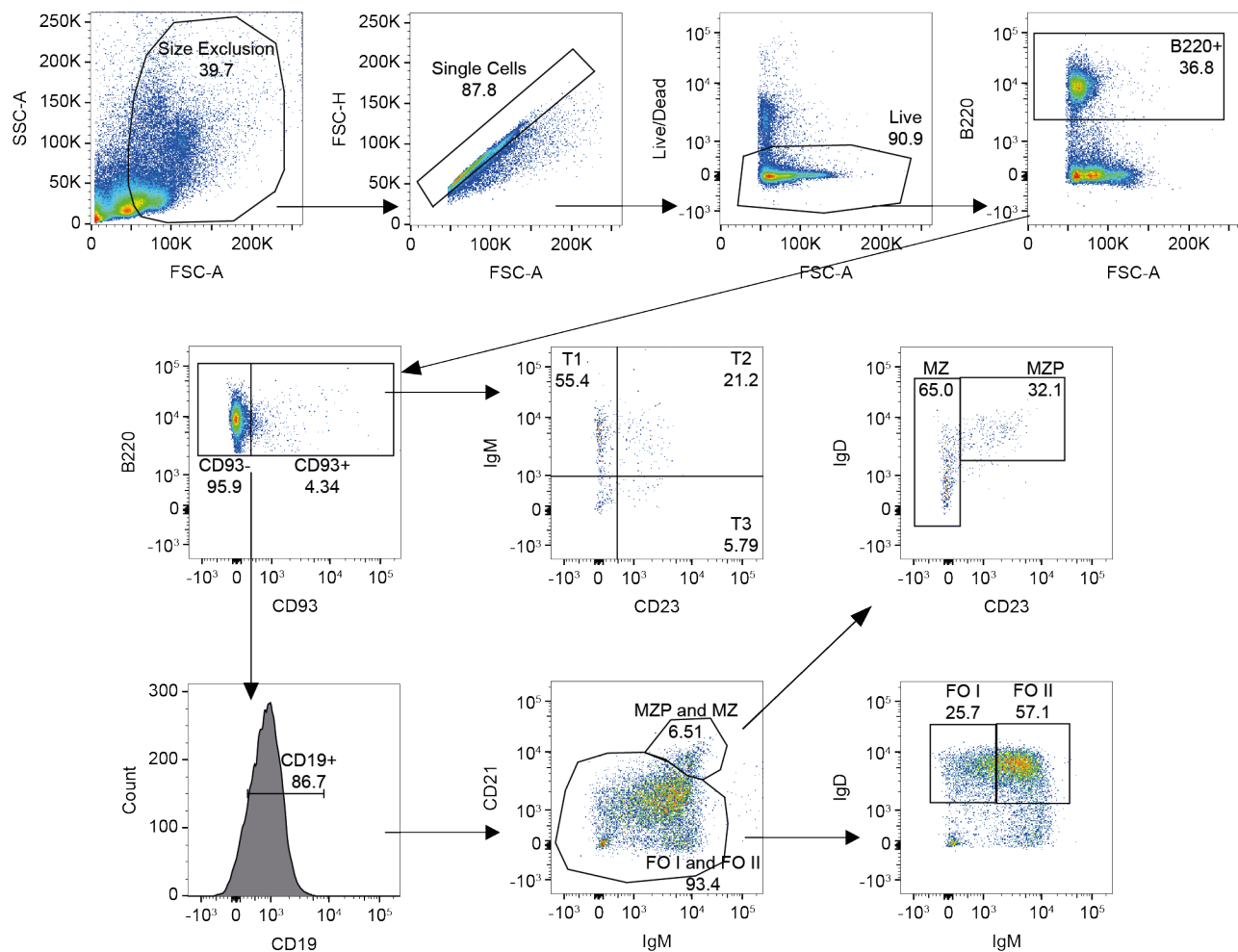
14



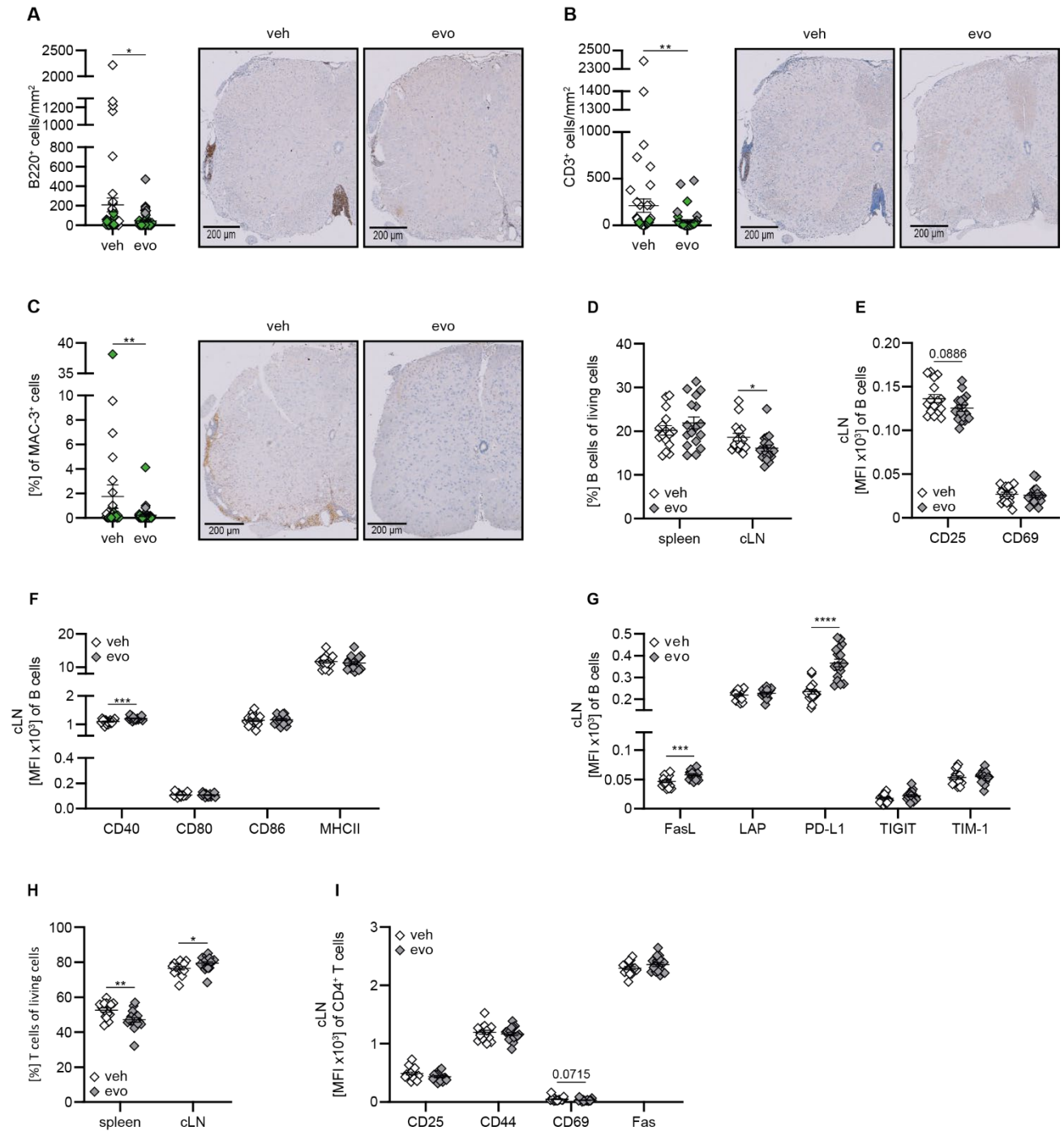
eFigure 2 Inhibition of BTK changes the composition of inflammatory and anti-inflammatory monocytes. A,B Frequency of Ly6C^{high} and Ly6C^{neg-low} M of living cells in spleen and cLN. **C-E** Frequency of plasmacytoid dendritic cells (pDCs, CD11c⁺Siglec H⁺), classical dendritic cells 1 (cDC1, CD11c⁺CD8⁺), and classical dendritic cells 2 (cDC2, CD11c^{high}CD11b⁺) of living cells in spleen and cLN. **F,G** Mean fluorescence intensity (MFI) of molecules associated with activation on CD4⁺ T cells isolated from the spleen and cLN. Data is shown as mean ± SEM; n=7-8 and representative data of two independent experiments. Asterisks indicate significant difference calculated using unpaired t test with Welch's correction or Mann-Whitney U test (*p<0.05, **p<0.01, ***p<0.001, ****p<0.0001).



eFigure 3 Gating strategy for analysis of murine immune cell composition. After exclusion of size, non-single cells and Zombie Dye positive cells, T cells were defined as CD3⁺ cells. CD3⁻ cells were further differentiated into CD19⁺ B cells and CD11b^{neg-pos} myeloid cells. The myeloid cells were further divided using CD11b and CD11c. CD11c⁺ cells were further divided into CD11c^{high}CD11b⁺ classical dendritic cells 2 (cDC2) and CD11c⁺CD11b^{pos-neg} cells into plasmacytoid dendritic cells (pDCs) as well as classical dendritic cells 1 (cDC1s). CD11b⁺ cells were further differentiated into neutrophils (CD11b⁺Ly6G⁺), eosinophils (CD11b⁺Ly6G⁻), and monocytes (CD11b⁺Ly6G⁻). Monocytes were differentiated into Ly6C^{high} and Ly6C^{neg-low} monocytes. Representative flow cytometric analysis of a spleen is shown for a naïve wild-type mice treated with 3 mg/ml evobrutinib for 21 days.

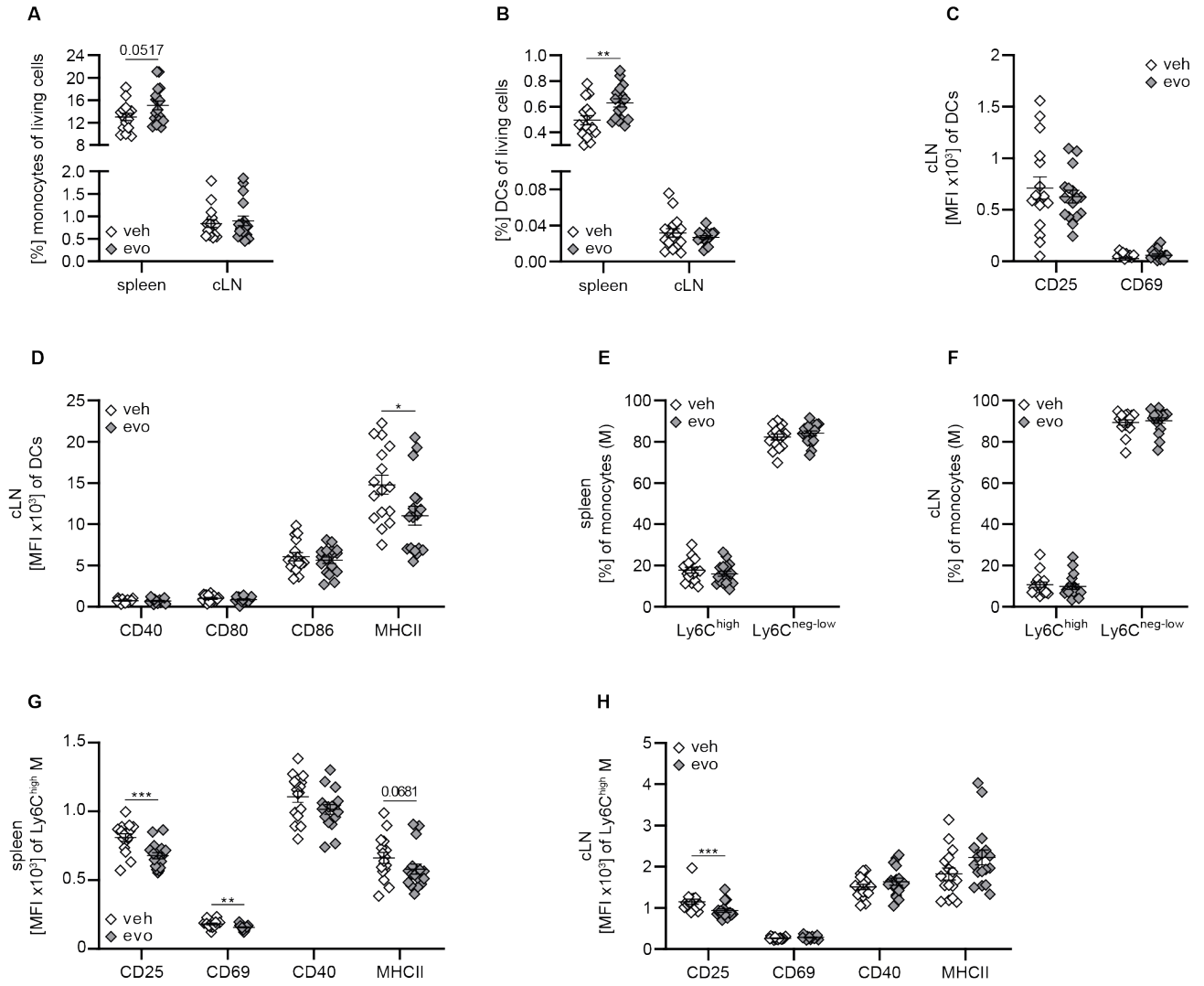


eFigure 4 Gating strategy for the analysis of B cell maturation. After exclusion of size, non-single cells and Zombie dye positive cells, the cells were gated based on their B220 expression. B220+ cells were then divided into CD93+ and CD93- cells. CD93+ cells were further characterized using CD19. CD19+ cells were separated into CD21+IgM+ marginal zone precursor B cells/marginal zone B cells (MZP/MZ) and follicular B cells. Marginal zone B cells are CD23- and IgDneg-pos whereas marginal zone precursor B cells are CD23+ but do not express IgD. Follicular B cells can be further divided into IgM+ follicular II (FO II) and IgM- follicular I (FO I) B cells. The CD93+ cell population was differentiated using IgM and CD23 into transitional B cell stages with T1 being IgM+CD23-, T2 IgM+CD23+ and T3 IgM-CD23+. Representative flow cytometry gating is shown for a spleen of a naïve wildtype mice treated with 3 mg/ml evobrutinib for 21 days.

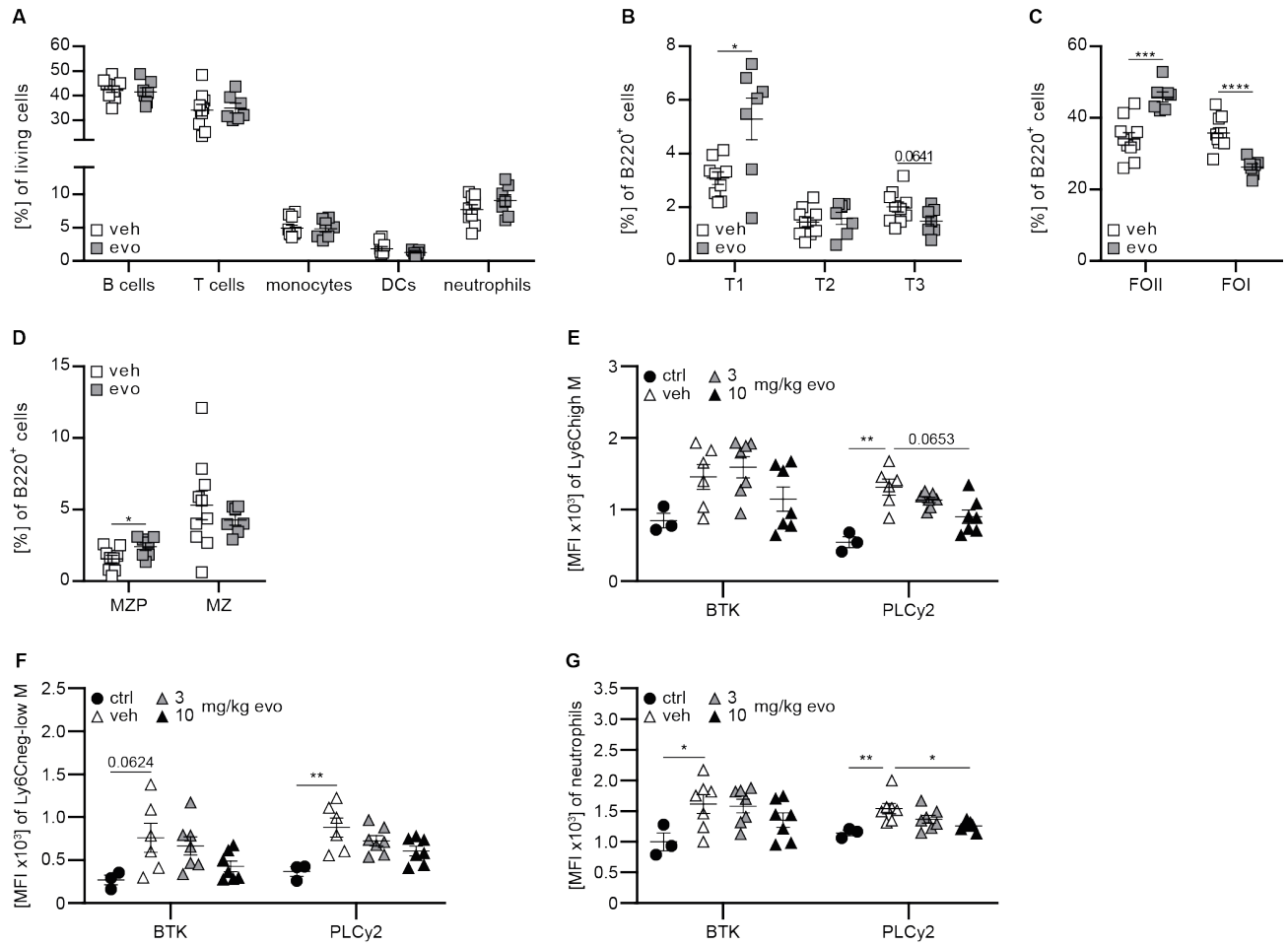


eFigure 5 BTKi reduces expression of activation and antigen presentation associated molecules on B cells in a spontaneous EAE model. Transgenic IgH^{MOG}xTCR^{MOG} mice were treated daily with 3 mg/kg evobrutinib (evo) or vehicle control (veh) starting at the age of 3.5 weeks. At the age of 10 weeks, immune cells of the spleen and cervical lymph nodes (cLN) were assessed using flow cytometry. Infiltration into the spinal cord of **A** B cells (B220⁺), **B** T cells (CD3⁺) and **C** macrophages (MAC3⁺). **D** Frequency of CD19⁺ B cells of living

cells in the spleen and cLN. **E-G** Mean fluorescence intensity (MFI) of surface molecules associated with activation, antigen presentation and regulation of B cells in the cLN. **H** Frequency of T cells (CD3⁺) of living cells in the spleen and cLN. **I** MFI of surface molecules associated with activation of CD4⁺ T cells in cLN. Data is shown as mean ± SEM; n=17 and representative data of two independent experiments. Asterisks indicate significant difference calculated using unpaired t test with Welch's correction or Mann-Whitney U test (*p<0.05, **p<0.01, ***p<0.001, ****p<0.0001).

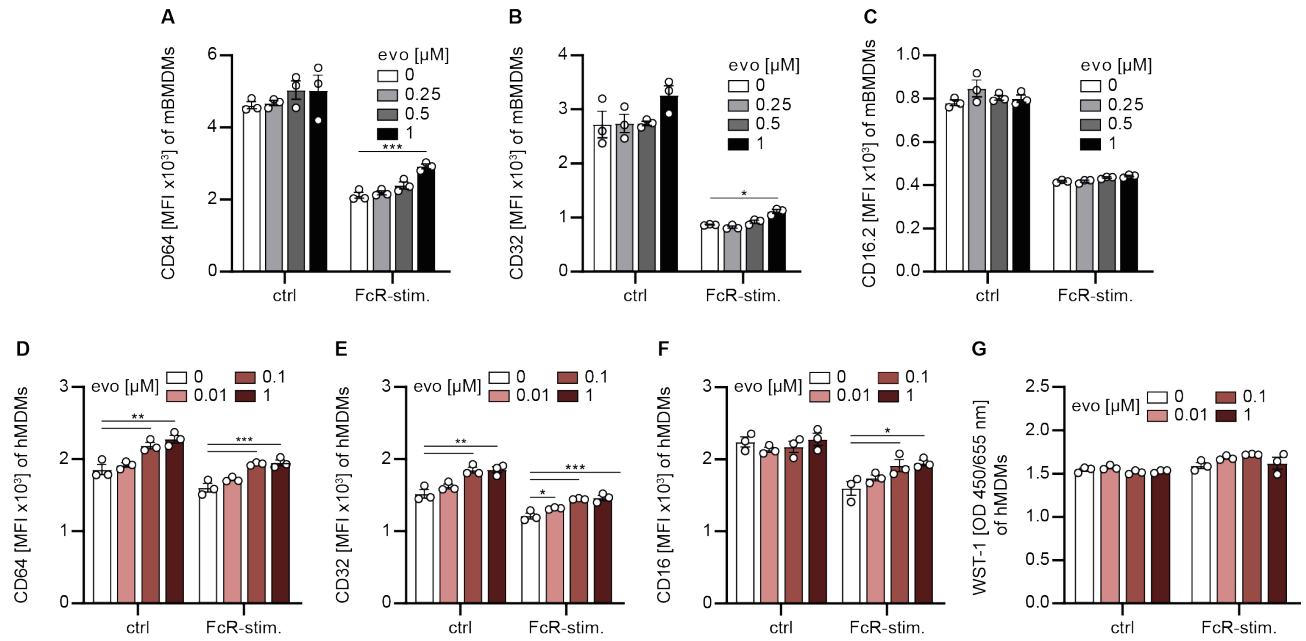


eFigure 6 BTKi lowers expression of molecules associated with activation and antigen presentation on myeloid cells in a spontaneous EAE model. Transgenic IgH^{MOG}xTCR^{MOG} mice were treated daily with 3 mg/kg evobrutinib (evo) or vehicle control (veh) starting at the age of 3.5 weeks. At the age of 10 weeks, immune cells of the spleen and cervical lymph nodes (cLN) were assessed using flow cytometry. **A** Frequency of CD11b⁺Ly6G⁻ monocytes (M) of living cells in the spleen and cLN. **B, D** Frequency of Ly6C^{high} and Ly6C^{neg-low} M of living cells in the spleen and cLN. **C** Mean fluorescence intensity (MFI) molecules associated with antigen presentation analyzed on Ly6C^{high} monocytes (M) in **C** spleen and **E** cLN. **F** Frequency of CD11b^{var}CD11c⁺ dendritic cells (DCs) of living cells in the spleen and cLN. MFI of surface molecules associated with **G** activation and **H** antigen presentation of DCs in cLN. Data is shown as mean \pm SEM; n=17 and representative data of two independent experiments. Asterisks indicate significant difference calculated using unpaired t test with Welch's correction or Mann-Whitney U test (*p<0.05, **p<0.01, ***p<0.001, ****p<0.0001).



eFigure 7 BTKi treatment ameliorates T cell-mediated CNS autoimmunity and suppresses myeloid activation, even without B cells.

A-D C57BL/6 mice were immunized with MOG₃₅₋₅₅ peptide, n=9. Mice were treated daily with either 3 mg/kg evobrutinib (evo) or vehicle (veh) starting 3 days prior to immunization. **A** Frequency of cell distribution in the spleen. **B** Frequency of Transitional T1, T2, T3 B cells in the spleen. **C** Frequency of Follicular FOII and FOI B cells in the spleen. **D** Frequency of marginal zone precursor (MZP) B cells a marginal zone (MZ) B cells. **E-G** B cell deficient μ MT mice were immunized with MOG₃₅₋₅₅ peptide, n=7. Mice were treated daily with either 3 mg/kg evo or veh starting 3 days prior to immunization. Day 5 post immunization, spleen was harvested and the activation of myeloid cells analyzed. MFI of BTK and PLC γ 2 expression of Ly6C^{high} and Ly6C^{neg-low} monocytes, and Ly6G⁺Ly6C⁺ neutrophils in the spleen. **A-D** unpaired t test with Welch's correction or Mann-Whitney U test (*p<0.05, **p<0.01, ***p<0.001, ****p<0.0001). **E-G** one-way analysis of variance corrected by Holm-Sidak or Kruskal-Wallis test with Dunn's multiple comparison of the treated groups to the vehicle control (*p<0.05, **p<0.01, ***p<0.001, ****p<0.0001).



eFigure 8 BTK inhibition enhances FcR expression of murine bone-marrow-derived macrophages (BMDMs) and human monocyte-derived macrophages (MDMs) *in vitro*, while showing no toxic effect. A-C Murine bone marrow-derived macrophages (BMDMs) were pre-activated with IFN- γ for 6 h. Afterwards, they were either cultured alone (ctrl) with evobrutinib (evo) for 18 h or in combination with FcR-stimulation and analyzed via flow cytometry. FcR-stimulation for 18 h in combination with evo. Mean fluorescence intensity (MFI) of CD64 (A), CD32 (B), and CD16.2 (C). D-G Human monocyte-derived macrophages (MDMs) were stimulated with FcR-stimulation for 18 h with different concentrations of evo. Mean fluorescence intensity (MFI) of CD64 (D), CD32 (E), and CD16 (F). G Cell viability was determined using WST-1 assay. Data sets are representative of at least three independent experiments, n=3. Data sets. The mean \pm SEM is indicated in all graphs; one-way analysis of variance corrected by Holm-Sidak or Kruskal-Wallis test with Dunn's multiple comparison of the treated groups to the control (*p<0.05, **p<0.01, ***p<0.001, ****p<0.0001).

eMethods

Sex as a biological variable

Female mice were used for all active EAE experiments. For all other experiments including the spontaneous EAE experiments, the MOG-IgG-mediated EAE, and the B cell deficient μ MT mice, both sexes male and female animals were examined, and similar findings are reported for male and female animals.

Evobrutinib treatment

Evobrutinib (Merck KGaA) was formulated in 20% Kleptose HPB (Merck KGaA) in 50 mM Na-Citrate buffer pH 3.0 and administered by oral gavage daily at 3 mg/kg body weight (BW) by oral gavage daily.

EAE induction and scoring

EAE induction of female wild-type mice using MOG₃₅₋₅₅ peptide was performed as described by Geladakis et al.^{e1}. To induce the MOG-IgG-mediated EAE by transfer of MOG-specific antibody, 150 μ g anti-MOG antibody (clone: 8.18C5) or isotype control antibody (clone: MOPC-21, Bio X cell) were injected into the tail vein of TCR^{MOG} recipients, twice a week up to a total of twelve injections. In this model, no immunization or adjuvant treatment was added. EAE severity was assessed daily according to Geladakis et al.^{e1}.

Preparation and digestion of 8.18C5

The preparation and digestion of the anti-MOG monoclonal antibody clone 8.18C5 was generated according to Kinzel et al.^{e2}.

Histology and immunohistochemistry

Histological and immunohistochemical analysis were performed as described by Hausler et al. extended by the analysis of Iba-1 (1:500; polyclonal; Fujifilm)³, respectively. Histological sections were captured using a digital camera (DP71; Olympus Europa) mounted on a light microscope (BX51; Olympus Europa) and a slideviewer (VS120 and VS200, Olympus Europa). Histological analysis was performed using QuPath-0.5.0 software (GitHub). At least 5 spinal cord cross sections per animal were taken for each analysis^{e3}.

Isolation of murine leukocytes

Single cell suspensions of from mouse lymphoid tissues were prepared by gentle dissection followed by passing through 70 µm cell strainer (Greiner Bio-One).

Generation of bone marrow-derived macrophages (BMDMs)

Generation of bone marrow-derived macrophages (BMDMs) was performed as described by Geladaris et al.^{e4}.

Assessment of T cell proliferation and activation *in vitro*

Adherent BMDMs were harvested using cell scraper, 0.5×10^5 cells/well were plated into 96-well flat-bottom plates and pre-stimulated with 100 ng/ ml IFN-γ for 6 h. Afterwards, BMDMs were washed with PBS and treated with evobrutinib and ovalbumin (OVA) protein overnight. After 24 h, 0.1×10^6 MACS purified (Pan T cell Isolation Kit, Miltenyi) -stained (CFSE Cell Division Tracker Kit, BioLegend) T cells from OT II mice were added per well. Every 24 h evobrutinib was added with the appropriate concentration. After 72 h co-culture, T cell proliferation and activation were evaluated by flow cytometry and ELISA.

Generation of human monocyte-derived macrophages (MDMs)

Peripheral blood mononuclear cells (PBMC) were isolated from human whole blood using the Ficoll-Paque density centrifugation methods. Monocytes were isolated by positive selection using CD14 MicroBeads (Miltenyi) according to manufacturer's instructions. Monocytes were cultured at 37 °C, 5 % CO₂ for 5 days in medium containing 50 ng/ml human M-CSF (AIM V™ medium, 10 % human serum, 50 U/ml penicillin, 50 µg/ml streptomycin) followed by 2 days in medium containing 10 ng/ml human IFN-γ (AIM V™ medium, 10 % human serum, 50 U/ml penicillin, 50 µg/ml streptomycin).

Nonliposomal transfection of plasmid DNA

For experiments with cell-bound human MOG, human embryonic kidney (HEK) 293-A cells (kindly provided by Dr. Markus Reindl, Innsbruck, Austria) were transfected with plasmid DNA encoding for the isoform α-1 of human MOG fused to

enhanced green fluorescent protein (EGFP). Purified pEGFP-N1-hMOG DNA was mixed with the nonliposomal transfection reagent FuGENE® HD (Promega) and DMEM. After incubation for 5 min at RT, the transfection mixture was added to the seeded HEK293-A cells. 48 h post transfection, the transfection efficiency was analyzed by fluorescence microscopy and cells were harvested for further experiments.

Cell-based assay

Human serum samples were analyzed for MOG-specific antibodies using cell-based assay (CBA). HEK293-A cells which stably expressed human MOG isoform α -1 or the control vectors (CV) on the surface were incubated with IgG or serum samples diluted 1:50 in medium for 15 min on ice. Cells were washed and APC-labeled goat anti-human IgG antibody was added for 15 min. Cells were analyzed by flow cytometry. The median fluorescence intensity was measured and the median ratio of HEK-MOG versus HEK-CV was calculated.

Evaluation of antigen uptake by myeloid APC

Adherent BMDMs were harvested using cell scraper, 0.5×10^5 cells/well were plated into 96-well flat bottom plates and pre-stimulated with 500 ng/ml lipopolysaccharide. 24 h thereafter, cells were incubated for 2 h with OVA-FITC (Life Technologies, Thermo Fisher Scientific) in the presence of 50 μ g/ml anti-OVA IgG1 Ab (clone: TOSG1C6, BioLegend) or isotype control Ab (clone: MOPC-21), and anti-OVA IgG2a Ab (clone: TOSGAA1, BioLegend) or isotype control Ab (clone: MOPC-173). Phagocytosis was quantified via flow cytometry.

Human MDMs were harvested using cell scraper, 0.5×10^5 cells/well were plated into 96-well round bottom plates and rested for 1 h at 37 °C. pEGFP-N1-hMOG-transfected HEK293-A cells were harvested using 0.05 % trypsin, 0.02 % EDTA (w/v) in PBS. MDMs were incubated for 2 h with transfected HEK293-A cells, in the presence of 0.5 mg/ml human serum. Phagocytosis was quantified via flow cytometry.

Cell activation assay with FcR-dependent stimulation

BMDMs were harvested using cell scraper, 0.5×10^5 cells/well were plated into 96-well flat bottom plates and pre-activated with 100 ng/ml IFN- γ for 6 h at 37 °C. BMDMs were then washed and cultured with appropriate concentrations

of evobrutinib in addition to 5 µg/ml Fc OxyBURST™ (Thermo Scientific) overnight. Next day, cells were detached using 0.05 % trypsin, 0.02 % EDTA (w/v) in PBS and stained for flow cytometric analysis. Supernatant was analyzed via ELISA for cytokine secretion. For analysis of intracellular proteins, cells were pre-treated with evobrutinib for 18 h followed by FcR-dependent stimulation with 40 µg/ml Fc OxyBURST™ (Thermo Scientific) for 15 min or 18 h and analyzed using flow cytometry.

MDMs were harvested using cell scraper, 0.5×10^5 cells/well were plated into 96-well round bottom plates and rested for 0.5 h at 37 °C. MDMs were pre-treated with evobrutinib for 0.5 h and then incubated with Fc receptor-dependent stimulation using 20 µg/ml Fc OxyBURST™ (Thermo Scientific) for 18 h. Surface expression was analyzed via flow cytometry. Cytokine release was analyzed via ELISA. For analysis of intracellular proteins, cells were pre-treated with evobrutinib for either 0. h followed by FcR-dependent stimulation with 40 µg/ml Fc OxyBURST™ (Thermo Scientific) for 15 min. Cells were analyzed using flow cytometry.

MDMs were harvested using cell scraper, 0.5×10^5 cells/well were plated into 96-well round bottom plates and rested for 0.5 h at 37 °C. pEGFP-N1-hMOG-transfected HEK293-A cells were harvested using 0.05 % trypsin, 0.02 % EDTA (w/v) in PBS. MDMs were pre-treated with 500 nM evobrutinib or vehicle for 1 h followed by cultivation with 0.64×10^5 cell/well non-transfected or transfected HEK293-A cells. Medium, control serum or MOG antibody positive serum (0.5 mg/ml) was added for 18 h. Supernatant was analyzed via ELISA for cytokine secretion.

ELISA for cytokine analysis

Production of murine IFN-γ, IL-6, TNF-α, and human IL-6, IL-10, TNF-α was measured using ELISA MAX Standard Set kits (BioLegend). Absorbance was measured at 450 nm with subtraction of a 540 nm reference wavelength on iMark microplate reader (Bio-Rad laboratories Inc.).

Cell viability

The WST-1 cell assay (Roche) was used to determine cell viability according to Geladaris et al.^{e4}.

Flow cytometry

Composition of murine immune cells was analyzed using the following antibodies: CD3 (145-2C11; BioLegend), CD8 (53-6.7; BioLegend), CD19 (6D5; BioLegend), CD11b (M1/70; BioLegend), CD11c (N418; BioLegend), Ly6C (HK1.4; BioLegend), Ly6G (1A8; BioLegend) and Siglec H (440C; BD Bioscience). B cell maturation was analyzed using the following antibodies: CD19 (6D5; BioLegend), CD21 (7G6; BD Bioscience), CD23 (B3B4; BD Bioscience), CD93 (AA4.1; BioLegend), CD45R/B220 (RA3-6B2; BioLegend), IgD (11-26c.2a; BioLegend), and IgM (AF6-78; BD Bioscience). Myeloid cell molecules involved in activation and antigen presentation were determined using: CD25 (3C7; BioLegend), CD40 (3/23; BD Bioscience), CD69 (H1.2F3; BioLegend), CD80 (16-10A1; BioLegend), CD86 (GL-1; BioLegend), and MHCII (2G9; BD Bioscience). Molecules with regulatory properties on B cells were analyzed using following antibodies: CD11b (M1/70, BioLegend), CD19 (6D5, BioLegend), CD39 (Y23-1185, BD Bioscience), CD45R/B220 (RA3-6B2, BioLegend), CD73 (TY/11.8, BioLegend), FasL/CD178 (REA1171, Miltenyi Biotec), LAP (TW7-16B4, BioLegend), PD-L1/CD274 (10F.9G2, BioLegend), TIGIT (1G9, BD Bioscience), Tim-1/CD365 (RMT1-4, BD Bioscience). T cell molecules involved in activation were determined using: CD3 (145-2C11, BioLegend), CD4 (GK1.5, BioLegend), CD25 (PC61.5, Invitrogen), CD44 (IM7, BioLegend), CD69 (H1.2F3, BioLegend), Fas/CD95 (Jo2, BD Bioscience). Bone marrow-derived macrophage molecules involved in antigen uptake and presentation were determined using: CD11b (M1/70, BioLegend), CD16.2 (9E9, BioLegend), CD32 (S17012B, BioLegend), CD40 (3/23, BD Bioscience), CD64 (X54-5/7.1, BioLegend), CD86 (GL-1, BioLegend), and MHCII (2G9, BD Bioscience). Monocyte-derived macrophage molecules involved in antigen uptake and presentation were determined using: CD11c (3.9, eBioscience), CD14 (MφP9, BD Bioscience), CD16 (B73.1, BioLegend), CD32 (FUN-2, BioLegend), CD40 (5C3, BioLegend), CD64 (10.1, BioLegend), CD86 (2331 (FUN-1), BD Bioscience), and MHCII (Tü36, BioLegend).

Fc receptors were blocked using monoclonal antibody specific for CD16/ CD32 (93; BioLegend). Dead cells were stained with a fixable viability kit (BioLegend). Samples were acquired on a BD LSR Fortessa (BD Bioscience). All data evaluation was performed using FlowJo software (FlowJo LLC).

Intracellular proteins were analyzed using the BD PhosFlow protocol and analyzed using the following antibodies: BTK (53/BTK; BD Bioscience), pBTK (N35-86, BD Bioscience), PLCγ2 (K86-1161, BD Bioscience).

References

- e1. Geladaris A, Torke S, Saberi D, et al. BTK inhibition limits microglia-perpetuated CNS inflammation and promotes myelin repair. *Acta Neuropathologica*. 2024;147(1)doi:10.1007/s00401-024-02730-0
- e2. Kinzel S, Lehmann-Horn K, Torke S, et al. Myelin-reactive antibodies initiate T cell-mediated CNS autoimmune disease by opsonization of endogenous antigen. *Acta Neuropathol*. Jul 2016;132(1):43-58. doi:10.1007/s00401-016-1559-8
- e3. Hausler D, Hausser-Kinzel S, Feldmann L, et al. Functional characterization of reappearing B cells after anti-CD20 treatment of CNS autoimmune disease. *Proc Natl Acad Sci U S A*. Sep 25 2018;115(39):9773-9778. doi:10.1073/pnas.1810470115
- e4. Geladaris A, Hausser-Kinzel S, Pretzsch R, et al. IL-10-providing B cells govern pro-inflammatory activity of macrophages and microglia in CNS autoimmunity. *Acta Neuropathol*. Apr 2023;145(4):461-477. doi:10.1007/s00401-023-02552-6